Journal of Magnetism and Magnetic Materials 395 (2015) 345–349

Contents lists available at ScienceDirect

Journal of Magnetism and Magnetic Materials

journal homepage: www.elsevier.com/locate/jmmm

Intrinsic dependence of the magnetic properties of $CoFe_2O_4$ nanoparticles prepared *via* chemical methods with addition of chelating agents

E.C. Mendonça [a], Mayara A. Tenório [b], S.G. Mecena [a], B. Zucolotto [a], L.S. Silva [a], C.B.R. Jesus [c], C.T. Meneses [a], J.G.S. Duque [a,*]

[a] Núcleo de Pós-Graduação em Física, Campus Prof. José Aluísio de Campos, UFS, 49100-000 São Cristóvão, SE, Brazil
[b] Departamento de Física, Campus Prof. Alberto Carvalho, UFS, 49500-000 Itabaiana, SE, Brazil
[c] Instituto de Física Gleb Wataghin, UNICAMP, C. P. 6165, 13083-970 Campinas, SP, Brazil

ARTICLE INFO

Article history:
Received 12 December 2014
Received in revised form
28 July 2015
Accepted 30 July 2015
Available online 31 July 2015

Keywords:
Chelating agents
Superparamagnetism
Co-precipitation

ABSTRACT

In this work, the effect of addition of different chelating agents on the magnetic properties of cobalt ferrite nanoparticles produced by the combining of both co-precipitation and hydrothermal methods is reported. The Rietveld analyses of X-ray diffraction patterns reveal that our samples are single phase (space group: *Fd-3m*) with small average sizes. The weight losses observed in the thermogravimetric measurements together with the $M \times H$ curves show that the organic contamination coming from chelating agent decomposition can give rise to misinterpretation of the magnetization measurements. Besides, analyses of the zero-field-cooled (ZFC) and field-cooled (FC) magnetization measurements and the $M \times H$ curves measured at room temperature allows us to state that both the average blocking temperature and particles size distribution are sensitive to the kind of chelating agent.

1. Introduction

The study of physical properties of nanoparticles systems and/or nanocomposites has attracted much attention due to both the appearing of new physical phenomena when compared with their bulk counterparts and the strong potential to technological applications [1–4]. However, from a point of view of material growth, the controlling of the morphological parameters such as particle sizes, shapes and size distribution is not an easy task. In order to reach such goal, chemical methods are the most used due mainly to the control of the kinetics parameters and the low cost. Such optimization is generally achieved using chemical addictive (generally organic compounds) [5–9]. However, the low temperatures generally used in these synthesis methods are not sufficient to eliminate completely the organic contamination of desired final product. In this scenario, this organic waste can play an important role in the analyses of the magnetization curves once the experimental data are generally normalized by the mass. In this sense, to avoid misinterpretations of the magnetization results, it is very important to know the true mass of magnetic material used in the analyses of the magnetization measurements.

In order to discuss this problem, we synthesize nanoparticles of $CoFe_2O_4$ by combining co-precipitation and hydrothermal techniques with the adding of the chelating agents: sucrose, glycerine, oleic acid and oleylamine plus sodium oleate. X-ray diffraction data show that the spinel phase was obtained for all samples. Once the crystallographic phase of the $CoFe_2O_4$ nanoparticles is formed at temperatures around 180 °C, the analysis of weight loss obtained from the thermogravimetric (TG) measurements allows us to conclude that samples are a mixing of organic waste and $CoFe_2O_4$ nanoparticles. Because of this, we have carried out a new mass normalization of the *MxT* and *MxH* curves. To estimate the magnetization saturation values, average size and size distribution of particle systems, the *MxH* loops measured at room temperature to three samples were fitted using a uniform magnetic model based on the Langevin function weight-averaged with a log-normal particle volume distribution.

2. Experimental procedure

$CoFe_2O_4$ nanoparticles were prepared from the mixing stoichiometric amounts of $Fe(NO_3)_3 \cdot 9H_2O$ and $Co(NO_2)_3 \cdot 9H_2O$ starting salts in distilled water which was gradually added to the mixture up to reaching the desired final volume. In order to evaluate the role of chelating agents in the magnetic properties, by

* Corresponding author.
E-mail address: gerivaldoduque@gmail.com (J.G.S. Duque).

http://dx.doi.org/10.1016/j.jmmm.2015.07.108
0304-8853/

combining the co-precipitation and hydrothermal methods, we have prepared four samples by adding the sucrose (0.02 mol/l), glycerine (0.02 mol/l), oleic acid (0.06 mol/l) and oleylamine (5 ml) plus sodium oleate (0.0002 mol/l). It is important to state that these chemical compounds were added to the aqueous solution under a constant mechanical stirring. After that NaOH solution was dropwise to keep a pH=13. The as-prepared mixture was sealed into a Teflon-lined stainless steel autoclave with a capacity of 110 mL for hydrothermal treatment at 180 °C during a time of 12 h to sucrose, glycerine, oleylamine plus sodium oleate and 2 h to oleic acid. Then, autoclave was cooled at room temperature and the precipitate was separated by centrifugation, washed with distilled water and absolute ethanol, and dried under open air at 50 °C. A detailed description of the synthesis procedure is given elsewhere [6,9,10].

The thermogravimetric measurements were recorded using a Q50 TA instruments in a temperature range $30 < T < 800$ °C. The room temperature X-ray diffraction data (XRD) were obtained with a Panalytical diffractometer with the Bragg-Brentano geometry in continuous mode with a scan speed of 1/4°/min in the 2θ range from 22° to 70° using CuK_α radiation. The Rietveld refinements were performed using the free software DBWS9807 [11,12]. The magnetization measurements as a function of the magnetic field and temperature were carried out using a superconducting quantum interference device (SQUID) magnetometer (Quantum Design MPMS evercool system).

3. Experimental results and discussion

Fig. 1 displays the thermogravimetric (TG) measurements carried out in the as-prepared samples from room temperature to 800 °C. The vertical arrows means the total loss weight and the dashed line indicates the temperature of the hydrothermal synthesis (T_a=180 °C). Interestingly, the greatest loss occurred to the sample prepared with two chelating agents. It is worth to emphasize that at this temperature the $CoFe_2O_4$ nanoparticles are already formed (see XRD data). The observed loss weights must be related with water evaporation (T~100 °C) and with decomposition of the chelating agents ($T > 200$ °C).

As one can see at 180 °C (see the dashed vertical line) only around 10% of total mass was lost and so we can conclude that our samples are a mixture of organic waste and ferrite cobalt

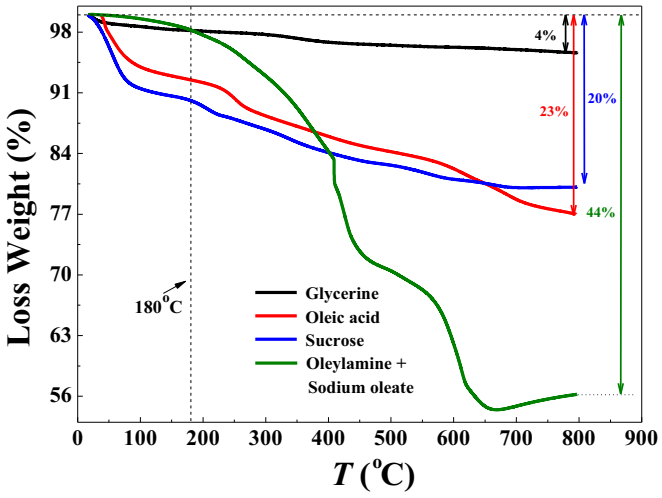

Fig. 1. Thermogravimetric (TG) measurements carried out to the as-prepared samples. The dashed vertical line indicates the temperature of the hydrothermal treatment and the vertical arrows represent the percentage of loss masses of samples.

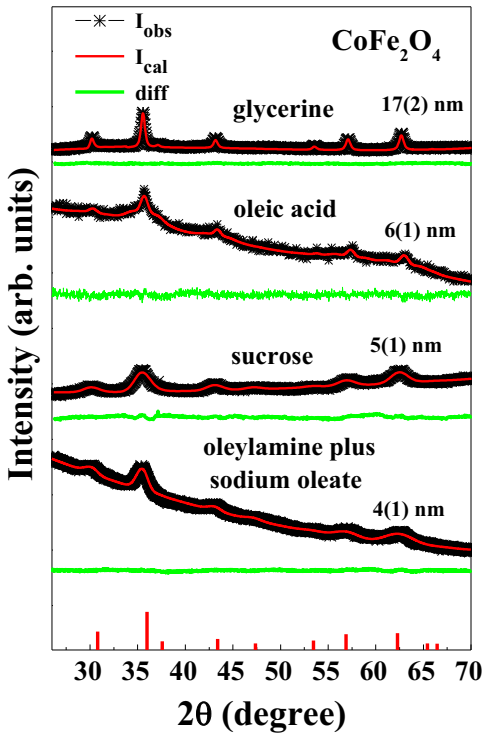

Fig. 2. X-ray diffraction data taken at room temperature to $CoFe_2O_4$ nanoparticles. The solid lines are the fittings using the Rietveld method (red lines) and difference (green lines) between the experimental and calculated patterns. The horizontal bars mean the standard pattern to $CoFe_2O_4$ (JCPDS Card 00-022-1086). (For interpretation of the references to color in this figure legend, the reader is referred to the web version of this article.)

nanoparticles. In order to confirm that all organic wastes are completely eliminated at 800 °C, samples were resubmitted to a second loop of TG and no loss weight was observed (not shown here).

According with TG results, to obtain the nanoparticles without the organic waste, one should increase the synthesis temperature to 800 °C. However, it is well known that the increasing of the annealing temperature generally results in the increasing of average nanoparticle sizes [13,14]. Indeed, this fact was observed in the XRD measurements performed in the samples after thermogravimetric measurements (not shown here). It is worth to mention that to obtain pure NiO nanoparticles by using a similar process Sasaki et al. [15] have used chemical additives to remove the organic waste.

Fig. 2 shows X-ray diffraction data taken at room temperature to $CoFe_2O_4$ nanoparticles. The solid lines mean the fitted patterns (red lines) and the difference between experimental and fitted patterns (green lines). The vertical bars mean the standard JCPDS card number 00-022-1086 to spinel crystalline structure of $CoFe_2O_4$.

Despite samples have been grown by using the same synthesis temperature, it is possible to observe differences in the peaks broadening which must be assigned to the chelating agents. For instance, one must clearly note that in the sample prepared with oleic acid seems to exist a superposition of broad and narrow peaks. Indeed, to fit the full width at half maximum of XRD patterns we have used the Thompson modified pseudo-voigth function which is one mixture of Gaussian and Lorentzian shapes. Such profile function takes account isotropic and anisotropic crystallite size and microstrain separately. The Rietveld refinement of XRD patterns confirm that our samples belong to the spatial group *Fd-3m*. Besides, except to the glycerine sample, the average particle size obtained from refinement seems to be chelating agent

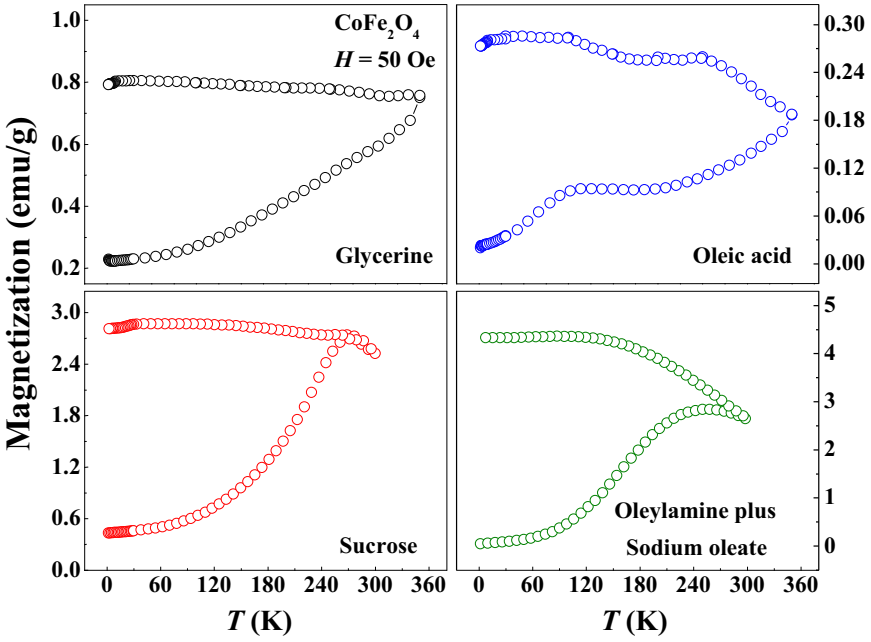

Fig. 3. Magnetization curves as a function temperature taken in zero-field-cooled (ZFC) and field–cooled (FC) mode at $H=50$ Oe to cobalt ferrite samples grown with sucrose, glycerine, oleic acid and oleylamine plus sodium oleate.

independent.

Fig. 3 presents the magnetization curves as a function temperature taken in zero-field-cooled (ZFC) and field-cooled (FC) mode at $H=50$ Oe to the cobalt ferrite nanoparticles grown with sucrose, glycerine, oleic acid and oleylamine plus sodium oleate. The values of magnetization are re-normalized by the mass of $CoFe_2O_4$ obtained from the TG analysis.

It is clear that the ZFC-FC curves yield different behaviors depending on the chelating agent. However, once the average particles size seems to be below a critical size to all used chelating agents (see XRD data), superparamagnetic features can be observed, that is, a maximum in the ZFC curves (except to glycerine sample) and an irreversible magnetic behavior. The maximum in ZFC curves observed to sucrose and oleylamine samples is, for noninteracting particles, directly proportional to the average blocking temperature which is associated with the mean particle size. On the other hand, while no maximum was observed to the glycerine sample, the oleic acid sample seems to present two maxima at $T_1=103$ K and $T_2>350$ K consistent with a bimodal distribution observed by Lopez-Dominguez et al. [17] to samples grown by using a similar procedure.

Interestingly, taking account that (i) our samples are a mixture of organic waste and $CoFe_2O_4$ nanoparticles and (ii) the loss weights observed in TG data increase sequentially as glycerine-sucrose-oleic acid-oleylamine, it is evident that there is an intrinsic dispersion effect of $CoFe_2O_4$ nanoparticles inside organic waste. Indeed, it notes that the peak of the ZFC curve displaces from ~270 K (sucrose sample) to ~250 K (oleic acid-oleylamine sample). However, the almost constant value of magnetization and the deviation from Curie-type behavior indicate that some interparticle interaction must be present [16].

If one supposes an assemble of noninteracting and spherical nanoparticles with uniaxial magnetic anisotropy, the blocking temperature calculated by the expression, $T_B \sim K_{eff}V/25\,k_B$ [18] with $d\sim5$ nm and $K_{eff}=2.5\times10^5$ J/m^3 (extracted from Ref. [19]) should be around 65.4 K to sucrose, oleic acid and oleylamine plus sodium oleate samples and 89.5 K to glycerine sample with $d\sim17$ nm and $K_{eff}=9.5$–12×10^3 J/m^3 (extracted from Ref. [20]). It must be observed that these values are not in agreement with that observed in the ZFC magnetization curves. However, the evaluation of the maximum value of the derivative of difference between ZFC and FC curves which is proportional to blocking temperature yields values closer to that the calculated using the above mentioned expression, 172 K and 234 K to oleylamine plus sodium oleate and sucrose samples, respectively. As we comment above, this disagreement can be indicating that some level of interparticle interaction is present, that is, the displacement of the peak position in the ZFC curves depends on the nanoparticle concentration inside the organic waste which affects the strength magnetic interaction between nanoparticles [16].

Fig. 4 shows the magnetization as a function magnetic field at room temperature to cobalt ferrite nanoparticles synthetized at $T_a=180$ °C. In the inset, we show the *MvsH* loops to the glycerine and oleylamine plus oleic acid samples before and after the normalization by the true mass of cobalt ferrite extracted from TG analysis. It is worth to remark that the evaluation of true mass of

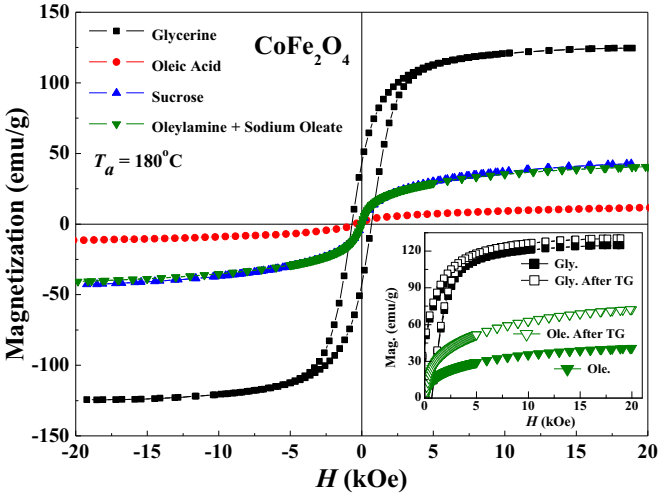

Fig. 4. Magnetization curves as a function magnetic field taken at room temperature to cobalt ferrite nanoparticles grown at $T_a=180$ °C. In the inset, we show the *MxH* loops to glycerine and oleylamine plus sodium oleate samples before (full symbols) and after (open symbols) the mass correction.

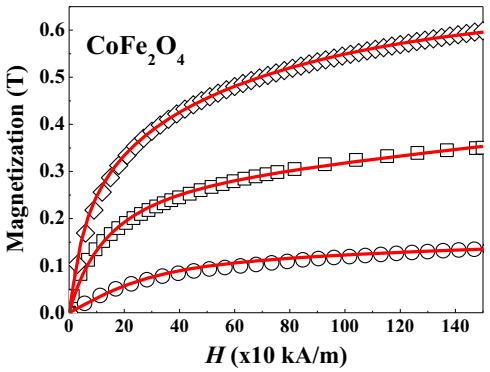

Fig. 5. *Fittings of the MxH curves* using the model described above to (○) oleic acid (□) sucrose and (◇) oleylamine plus sodium oleate samples.

nanoparticles was extracted from the percentage of total mass loss obtained from TG data (see Fig. 1).

One must note that while in the glycerine sample the saturation magnetization remained almost the same after mass correction, the oleylamine plus oleic acid sample presents an appreciable change in the saturation magnetization increasing from 40.5 to 72.2 emu/g. Many works in literature [5,13,21–24] which report on the magnetic properties of magnetic nanoparticles obtained *via* chemical methods with chelating agents discuss the changes in the magnetization saturation when compared with its bulk value as an effect coming from particles surface. We also agree with such interpretation, however, in this scenario, we want to call attention that the crude magnetization curves of the samples grown *via* chemical route with chelating agents can drive to the misinterpretations.

Once, at room temperature, no coercivity is observed in the $M \times H$ loops to sucrose, oleic acid and oleylamine plus sodium oleate samples, we believe that these samples are in the superparamagnetic state, that is, thermal agitation is dominant when compared with another effects. In this sense, some works in literature [17,18,25–30] have used a generalized model to fit magnetization curves as function of magnetic field in the superparamagnetic state. It is well known that the magnetic behavior of superparamagnetic nanoparticles with uniaxial anisotropy axis is governed by magnetization reversal processes, that is, magnetic moments inside nanoparticles can rotate collectively under action of both thermal agitation and/or magnetic field. On the other hand, to real system, the size distribution is another important feature that can influence the magnetic response of the system. In order to estimate the mean size and size distribution nanoparticles from the $M \times H$ curves, following a procedure found in Refs. [17,18], we have used a uniform magnetic model based on the Langevin function weight-averaged with a log-normal particle volume distribution. In Fig. 5, we show $M \times H$ curves fitted by such simple model to the sucrose, oleic acid and oleylamine plus sodium oleate samples. As one can see, there is a good agreement between the experimental and fitted data. Unfortunately, we are not able to fit the sample grown with glycerine once the coercive field is not zero. By assuming that our samples present a size distribution represented by a log-normal function:

$$p(V;\sigma,V_0)=\frac{1}{\sigma V\sqrt{2\pi}}\exp\left(-\frac{\ln\frac{V}{V_0}}{2\sigma^2}\right) \quad (1)$$

where $V_0=\frac{\pi D_0^3}{6}$ is the particle average volume, we have computed the magnetization as function of the magnetic field using the following equation:

Table 1
Parameters extracted from the fittings of *MxH* and X-ray diffraction data to the samples growth with sucrose, glycerine, oleic acid and oleylamine plus sodium oleate.

	Mean size (nm) XRD	Mean size (nm) model	σ Model	M_S (emu/g) model	χ_{pm} ($\times 10^{-8}$)
Sucrose	5(1)	5.0	1.1	43.7	5.24
Glycerine	17(3)	–	–	–	–
Oleic Acid	6(1)	5.4	0.9	14.4	0.61
Oleylamine	4(1)	4.9	1.1	89.8	4.11

$$M(H)=\int_0^\infty p(V;\sigma,V_0)\left[M_S L(x)+\chi_{pm}H\right] \quad (2)$$

where L is one Langevin function with $x=\frac{\mu_0 M_S V H}{k_B T}$.

Table 1 shows the parameters extracted from the best fits by using the uniform model. One can see that there is a good accordance of the average particles size estimated by XRD data with that calculated *via* model. These analysis show that independently of the used chelating agent, the fitted samples present a small size and size distribution (approximately $<D>=5$ nm and $\sigma=1$).

4. Conclusions

$CoFe_2O_4$ nanoparticles were synthesized by combining co-precipitation and hydrothermal chemical methods with addition of different chelating agents. The analyses of the XRD patterns are consistent with a cubic structure belonging to the *Fd-3m* space group to all samples. Thermogravimetric data show strong loss masses which increases sequentially as glycerine-sucrose-oleic acid-oleylamine. Besides, despite chelating agents can help us in the control of important morphologic parameters such as size, shape and size distribution, we show that organic contamination coming from decomposition of chelating agents which is present in samples after synthesis procedure can drive to misinterpretations of the magnetization data. Finally, by using a uniform model to fit magnetization *vs* magnetic field curves at room temperature we conclude that our samples present a small mean size and size distribution.

Acknowledgments

We thank FAPITEC/SE and CNPq for financial support.

References

[1] M. Sugimoto, J. Am. Ceram. Soc. 82 (1999) 269.
[2] S.A. Shah, M.H. Asdi, M.U. Hashmi, M.F. Umar, Saif-Ullah Awan, Mater. Chem. Phys. 137 (2012) 365.
[3] O.M. Lemine, K. Omri, M. Iglesias, V. Velasco, P. Crespo, P. de la Presa, L. el Mir, H. Bouzid, A. Yousif, A. Al-Hajry, J. Alloy. Compd. 607 (2014) 125.
[4] C. Jean-Paul Fortin, J. Wilhelm, C. Servais, Jean-Claude Bacri Menager, F. Gazeau, J. Am. Chem. Soc. 129 (2007) 2628.
[5] V. Lopez-Dominguez, J.M. Hernandez, J. T, R.F. Ziolot, Chem. Mater. 25 (2013) 6.
[6] Shao-Yun Xing-Hua Li, Fub, Lu-Ping Zhu, Nanoscale Res. Lett. 5 (2010) 1039.
[7] T.G. Altincekic, I. Boz, A. Baykal, S. Kazan, R. Topkaya, M.S. Toprak, J. Alloy. Compd. 493 (2010) 493.
[8] C.I. Covaliu, I. Jitaru, G. Paraschiv, E.V. Sorin-Stefan Biris, L. Diamandescu, V. Ionita, H. Iovu, Powder Technol. 237 (2013) 415.
[9] S. Gyergyek, M. Drofenika, D. Makovec, Mater. Chem. Phys. 133 (2012) 515.
[10] R.J.S. Lima, J.R. Jesus, K.O. Moura, C.B.R. Jesus, J.G.S. Duque, et al., J. Appl. Phys. 109 (2011) 123905.
[11] L. Bleicher, J.M. Sasaki, C.O. Paiva-Santos, J. Appl. Crystallogr. 33 (2000) 1189.
[12] R.A. Young, A. Sakthivel, T.S. Moss, C.O.J. Paiva-Santos, Appl. Crystallogr. 28 (1995) 366.
[13] K. Maaz, S. Karim, A. Mumtaz, S.K. Hasanain, J. Liu, J.L. Duan, J. Magn. Magn. Mater. 321 (2003) 1838.

[14] S. Briceno, W. Bramer-Escamilla, P.S. Gerzon, E. Delgado, E. Plaza, J. Palacios, E. Canizales, J. Magn. Magn. Mater. 324 (2012) 2926.
[15] N.S. Gonçalves, J.A. Carvalho, Z.M. Lima, J.M. Sasaki, Mater. Lett. 72 (2012) 36.
[16] R.D. Zysler, D. Fiorani, A.M. Testa, J. Magn. Magn. Mater. 224 (2001) 5.
[17] Joan Manel Victor Lopez-Dominguez, Javier Hernàndez, Tejada, Ronald F. Ziolo, Chem. Mater. 25 (2013) 6.
[18] F.C. Fonseca, G.F. Goya, R.F. Jardim, R. Muccillo, N.L.V. Carreno, E. Longo, E. R. Leite, Phys. Rev. B 66 (2002) 104406.
[19] V. Blaskov, V. Petkov, V. Rusanov, Ll. M. Martinez, B. Martinez, J.S. Mufioz, M. Mikhov, J. Magn. Magn. Mater. 162 (1996) 331.
[20] C. Cannas, A. Musinu, G. Piccaluga, D. Fiorani, D. Peddis, H.K. Rasmussen, S. Mørup, J. Chem. Phys. 125 (2006) 164714.
[21] Shao-Yun Xian-Ming Liu, Fu, Lu-Ping Zhu, J. Solid State Chem. 180 (2007) 461.
[22] S.K. Sharma, J.M. Vargas, E. De Biasi, F. Beron, M. Knobel, K.R. Pirota, C. T. Meneses, S. Kumar, C.G. Lee, P.G. Pagliuso, C. Rettori, Nanotechnology 21 (2010) 035602.
[23] E. Lima Jr., E. De Biasi, M.V. Mansilla, M.E. Saleta, F. Effenberg, L.M. Rossi, R. Cohen, H.R. Rechenberg, R.D. Zysler, J. Appl. Phys. 108 (2010) 103919.
[24] R.D. Zysler, M.V. Mansilla, D. Fiorani, Eur. Phys. J. B 41 (2004) 171.
[25] K. Yakushiji, S. Mitani, K. Takanashi, J.-G. Ha, H. Fujimori, J. Magn. Magn. Mater. 212 (2000) 75.
[26] R.W. Chantrell, J. Popplewell, S.W. Charles, IEEE Trans. Magn. 14 (1978) 975.
[27] R.C. Woodward, J. Heeris, T.G. Pierre St., M. Saunders, E.P. Gilbert, M. Rutnakornpituk, Q. Zhange, J.S. Riffle, J. Appl. Crystallogr. 40 (2007) s495.
[28] A. Millana, A. Urtizberea, N.J.O. Silva, F. Palacio, V.S. Amaral, E. Snoeck, V. Serinc, J. Magn. Magn. Mater. 312 (2007) L5.
[29] J. Popplewell, L. Sakhnini, J. Magn. Magn. Mater. 149 (1995) 72.
[30] J. Vejpravová, V. Sechovský, J. Plocek, D. Nižanský, A. Hutlová, J.-L. Rehspringer, J. Appl. Phys. 97 (2005) 124304.